Sliding Mesh Simulation of Laminar Flow in Stirred Reactors

André Bakker
Richard D. LaRoche
Min-Hua Wang
Richard V. Calabrese

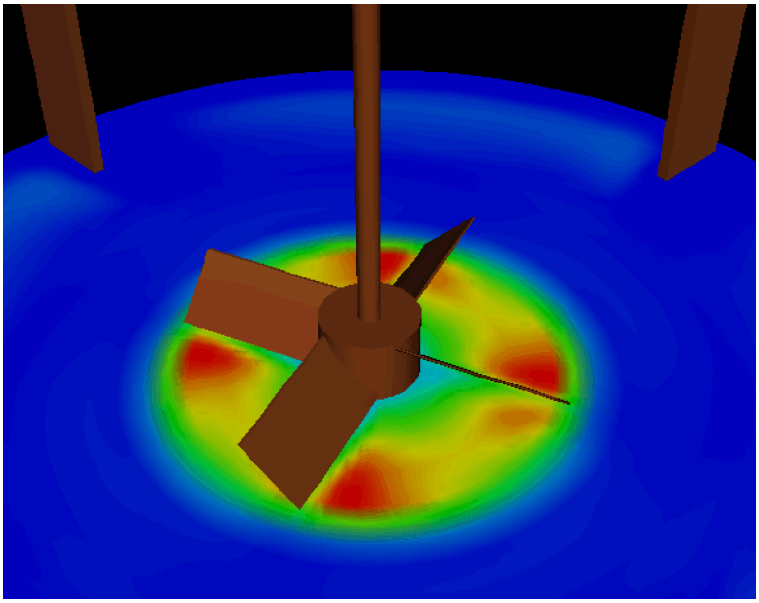

The flow pattern created by a pitched blade turbine was calculated using a sliding mesh method for various Reynolds numbers, mostly in the laminar regime. This method allows flow pattern calculations without the use of any experimental boundary conditions. The results compared favorably with experimental data obtained by laser-Doppler velocimetry. At low Reynolds number the impeller creates a radial flow pattern, rather than axial. The pumping number decreases with decreasing Reynolds number. It is concluded that the sliding mesh method is suitable for the prediction of flow patterns in stirred tanks.

Keywords: Stirred Tank, Sliding Mesh, Impeller, Mixing, Laminar Flow
Published in "The Online CFM Book" at http://www.bakker.org/cfm.
 Updated: February 15, 2000

INTRODUCTION

Computational fluid dynamics models are now regularly used to calculate the flow patterns in stirred reactors. To model the impeller, it is common to prescribe experimentally obtained velocity data in the outflow of the impeller, see e.g. Bakker and Van den Akker [1]. This has the disadvantage that it is often necessary to extrapolate the data to situations for which no experiments were or can be performed. Only recently have methods become available to explicitly calculate the flow pattern around the impeller blades without prescribing any experimental data. The presence of baffles complicates such calculations, as they remain stationary while the impeller rotates. The sliding mesh method is a novel way of dealing with the impeller-baffle interaction. The main advantage of the sliding mesh method is that no experimentally obtained boundary conditions are needed, as the flow around the impeller blades is being calculated in detail. This allows modeling of impeller systems and reactors for which experimental data is difficult or impossible to obtain. The purpose of this paper is to report on initial studies to the suitability of this novel method for the prediction of the flow pattern in stirred tanks. We will first discuss the background of the sliding mesh method, and then present computational results and a comparison with experimental data.

SLIDING MESH METHOD

With the sliding mesh method the tank is divided in two regions that are treated separately: the impeller region and the tank region that includes the bulk of the liquid, the tank wall, the tank bottom and the baffles, see Figure 1.

The grid in the impeller region rotates with the impeller. The grid in the tank remains stationary. The two grids slide past each other at a cylindrical interface. Here only a 90^o section of the tank is modeled, using a cyclic boundary condition at the sides.

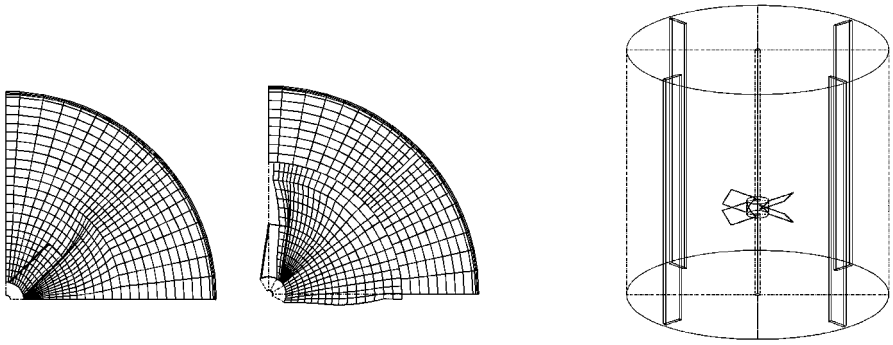

Figure 1 *Grid used in the sliding mesh method. The grid is shown at two different time steps. The grid in the impeller region moves with the impeller and slides past the stationary grid for the rest of the tank. The impeller is a pitched blade turbine with four blades at a 45^o angle.*

In the tank region the standard conservation equations for mass and momentum are solved. In the rotating impeller region a modified set of balance equations is solved:

$$\frac{\partial}{\partial x_j}(u_j - v_j) = 0$$

$$\frac{\partial}{\partial t}\rho u_i + \frac{\partial}{\partial x_j}\rho(u_j - v_j)\,u_i = -\frac{\partial p}{\partial x_i} + \frac{\partial \tau_{ij}}{\partial x_j} \qquad (1)$$

Here u_j is the liquid velocity in a stationary reference frame and v_j is the velocity component arising from mesh motion. Further p is the pressure and τ_{ij} is the stress tensor. The first equation is the modified continuity equation and the second equation is the modified momentum balance.

At the sliding interface a conservative interpolation is used for both mass and momentum, using a set of fictitious control volumes. No-slip boundary conditions are used at the impeller blades, the shaft, the baffles and the tank walls. No experimental data is prescribed in the outflow of the impeller. All fluid motion strictly arises from the rotation of the impeller blades. The grid was generated with a proprietary program named AgFlow from Chemineer, Inc. The total number of grid nodes was approximately 49000. All simulations were performed using Fluent™ from Fluent, Inc. More details of the numerical methods can be found in Murthy *et al.* [2] and in reference [3].

SIMULATION

Time dependent simulations were performed for the flow created by a pitched blade turbine in a tank with a diameter of T = 0.3 m. The impeller diameter was D = T/3 and the impeller to bottom clearance was C = T/3. The blade width was W = 0.2 D and the blades were set at a 45^o angle with the horizontal. The tank was equipped with four baffles, T/12 wide and T/72 offset from the tank wall. The impeller rotational speed was N = 3.75 s^{-1} and the viscosity was varied to obtain impeller Reynolds numbers ($Re = \rho.N.D^2/\mu$) ranging from Re = 17 to Re = 1200. In this range the flow was laminar. In addition one simulation was performed for a Reynolds number of 10000 where the flow was turbulent, mainly to obtain an impeller pumping number for comparative purposes. In that case the k-ε RNG turbulence model was used [3].

In the simulations a time step of 0.01 s was used and up to 1000 time steps were performed, resulting in 37.5 revolutions. Local and average velocities were tracked as a function of time to determine when periodic steady state was reached. The local velocities close to the impeller converged fastest, while the average tangential velocity in liquid bulk converged slowest. The number of revolutions to achieve periodic steady state increased from about 15 for Re = 40 to about 35 for Re = 1200, as illustrated in Figure 2.

Calculation time is approximately 15 minutes per impeller revolution on a Cray C-90 computer. The experimental velocity data of Wang *et al.* [4], acquired via laser-Doppler velocimetry, was used for validation of the computational results.

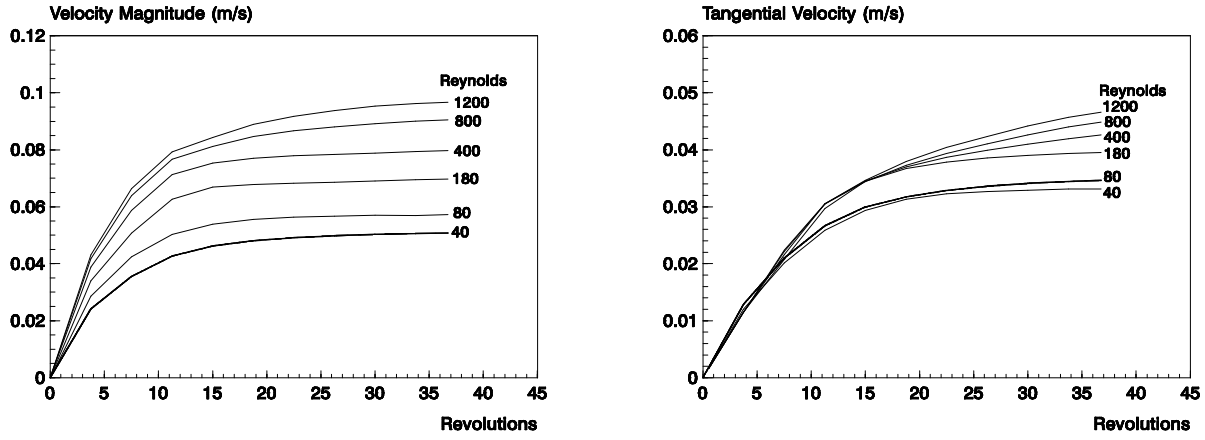

Figure 2 *The average velocity magnitude in the vessel as a function of Reynolds number and number of revolutions is shown on the left. The average tangential velocity in the vessel is shown on the right. The number of revolutions needed to achieve steady state increases with Reynolds number, as do the velocities. The tangential velocity typically converges slower than the other velocity components.*

RESULTS

Figure 3 shows the velocity field for a Reynolds number of 40. The flow pattern is shown by means of velocity vectors. The vectors point in the direction of the liquid velocity at the point where they originate. The length of the vectors is proportional to the magnitude of the liquid velocity. The experimentally measured velocities are shown on the left while the sliding mesh results are shown on the right. At this Reynolds number the impeller creates a mainly radial flow pattern. Two circulation loops form, above and below the impeller. The flow is very weak away from the impeller. The model results can be seen to compare quite well with the experimental data. At low Reynolds numbers the flow was predominantly radial as shown here.

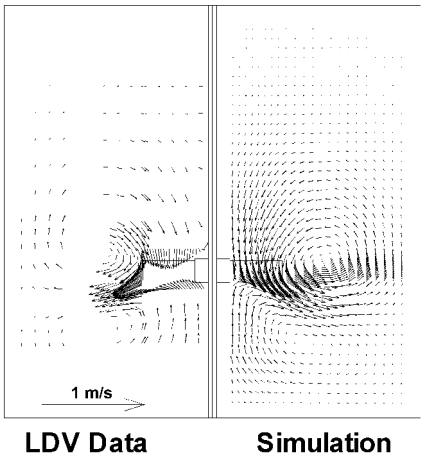

Figure 3 *Comparison between experimental data (left) and sliding mesh results (right). The impeller Reynolds number is 40.*

However, for Reynolds numbers larger than 400 the jet coming from the impeller hit the tank bottom rather than the wall and the flow was more axial. Figure 4 shows how the flow pattern becomes more axial as the Reynolds number increases.

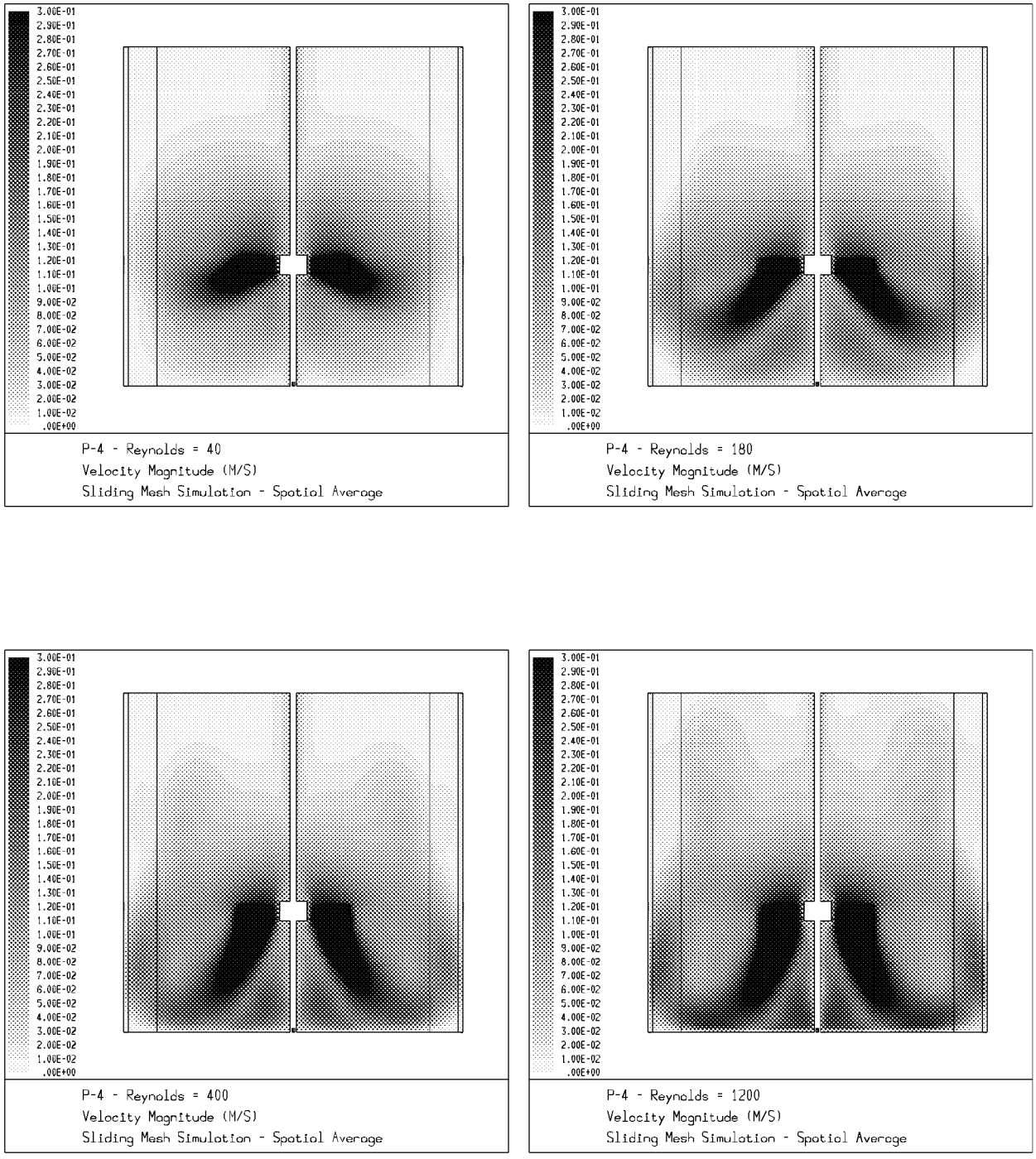

Figure 4 *Local velocity magnitude as a function of Reynolds number, for a constant impeller rotational speed but varying liquid viscosity. The flow pattern becomes more axial and the velocity magnitude increases as the Reynolds number increases.*

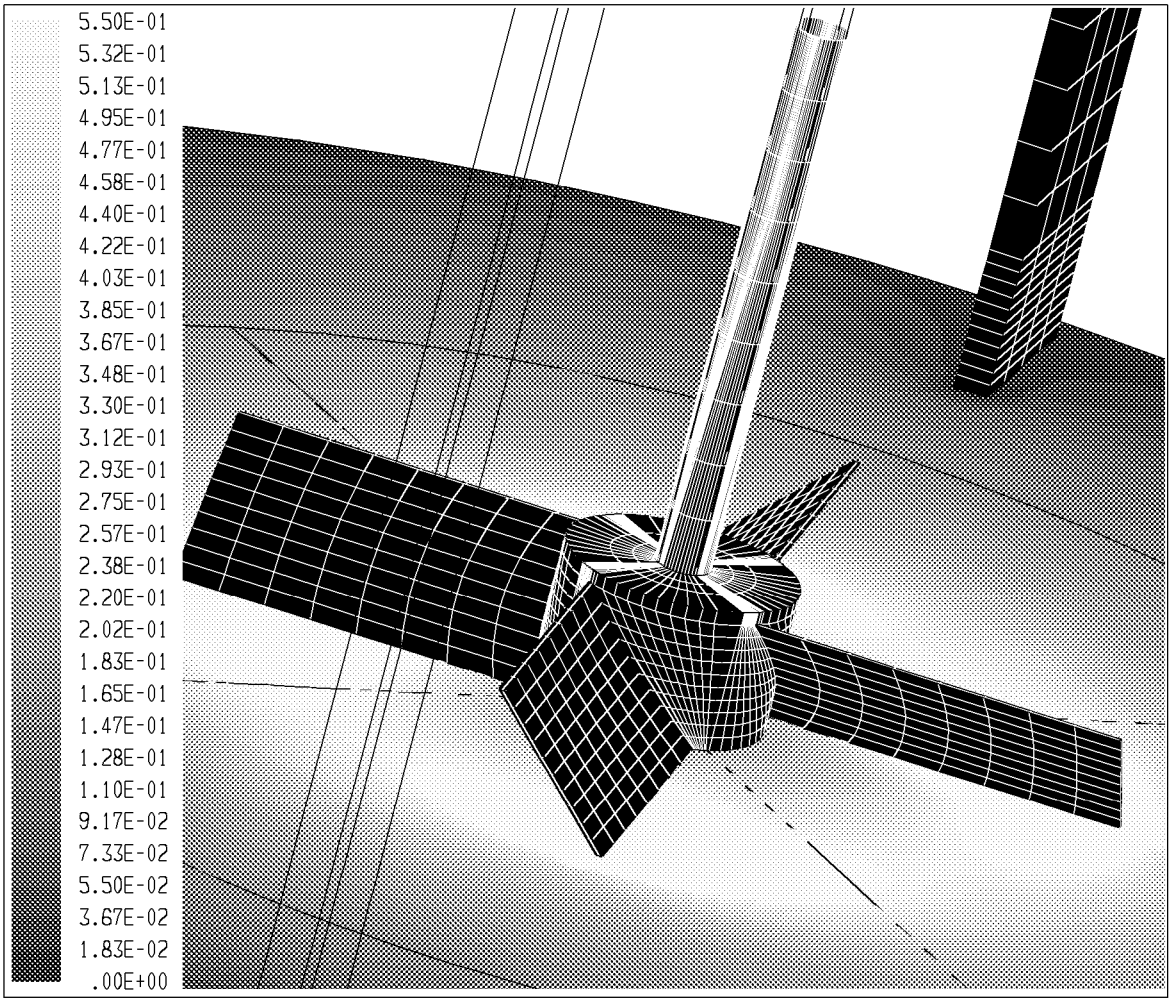

Figure 5 *Local velocity magnitude in a plane just below the impeller for Re = 40. The grid at the impeller blade and at the baffle is also shown.*

Figure 5 shows the local velocity magnitude in a plane just below the impeller for a Reynolds number of 40. Light colored regions denote high velocities, while dark colored regions denote low velocities. The highest velocities are found near the impeller blade tip. The velocities are lowest near the baffle. This figure also shows the grid at the impeller blade. Under the laminar flow conditions studied here, this grid density seems to be sufficient. However, it is anticipated that under turbulent flow conditions a finer grid will be necessary to resolve the effects of possible turbulent tip vortices.

For a more quantitative validation the impeller pumping number $N_q = Q_l/N.D^3$ was calculated, both from the experimental data from Wang *et al.* [4] and from the sliding mesh data. The pumping rate Q_l includes both the radial flow at the side of the impeller and the axial flow at the bottom of the impeller. Figure 4 shows the pumping number as a function of Reynolds number. There is good quantitative comparison between the simulation results and the experimental data. As expected, the pumping number decreases significantly with decreasing Reynolds number.

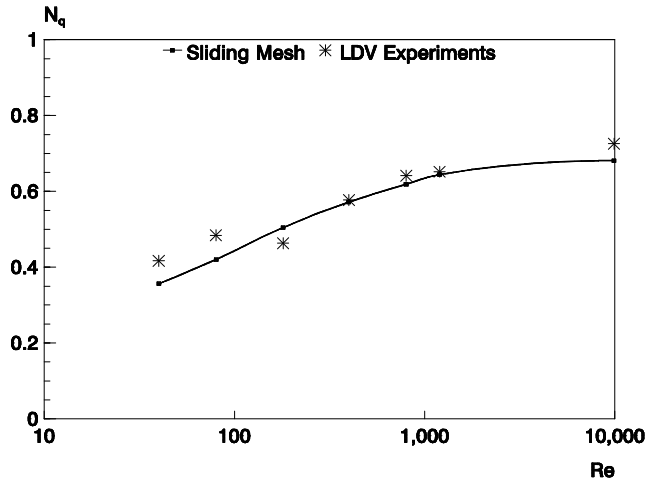

Figure 6 *Comparison between experimental data and sliding mesh results for the impeller pumping number as a function of impeller Reynolds number. The pumping number was calculated based on the total liquid flow rate leaving the impeller.*

DISCUSSION

Sliding mesh methods can be used to accurately predict the time dependent laminar flow pattern in stirred reactors, without the need for experimental data as impeller boundary conditions. A drawback is the long calculation time which is about an order of magnitude longer than with steady state calculations based on experimental impeller data.

Further testing and validation of these models for turbulent flow conditions is necessary. Furthermore, grid dependency studies will have to be performed to determine the minimum grid resolution necessary to resolve turbulent tip vortices.

An important application for the sliding mesh method might be the development of new, optimized impeller designs for specific industrial applications. Other applications are the prediction of flow patterns with impellers for which no experimental data are available, the prediction of flow patterns in multiple impeller systems where there is significant interaction between the impellers and to predict time dependent flow patterns in systems where steady state assumptions are not justified.

REFERENCES

[1] Bakker A., Van den Akker H.E.A. (1994)
Single-Phase Flow in Stirred Reactors
Chemical Engineering Research and Design, TransIChemE Vol. 72, Number A4, July 1994, page 583-593.

[2] Murthy J.Y., Mathur S.R., Choudhury D. (1994)
CFD Simulation of Flows in Stirred Tank Reactors Using a Sliding Mesh Technique
Mixing 8, Proceedings of the Eighth European Conference on Mixing, Institution of Chemical Engineers, Symposium Series No. 136, page 341-348, ISBN 0 85295 329 1

[3] Fluent User's Guide, Fluent, Inc., (1995)

[4] Wang M.H., Calabrese R.V., Bakker A. (1995)
Effect of Reynolds Number on the Flow Generated by a Pitched Blade Turbine
Presented at the 45th CSChE Conference, Québec City, October 15-18, 1995

NOTATION

D	Impeller Diameter	(m)
N	Impeller Rotational Speed	(s^{-1})
N_q	Impeller Pumping Number	(-)
Q_l	Flow Rate	($m^3 s^{-1}$)
p	Pressure	(N m^{-2})
Re	Impeller Reynolds Number	(-)
T	Tank Diameter	(m)
u_j	Liquid Velocity in Direction j	(m s^{-1})
v_j	Mesh Velocity in Direction j	(m s^{-1})
W	Impeller Blade Width	(m)
τ_{ij}	Molecular Shear Stress	(kg m^{-1} s^{-2})
ρ	Liquid Density	(kg m^{-3})
μ	Viscosity	(Pa s)